

AD-A048 018

WEAPONS RESEARCH ESTABLISHMENT SALISBURY (AUSTRALIA)  
ROCKET BORNE OBSERVATION OF ELECTRON DENSITY DURING A TRAVELLIN--ETC(U)  
JUN 77 K H LLOYD, C J BEACH  
WRE-TR-1028(W)

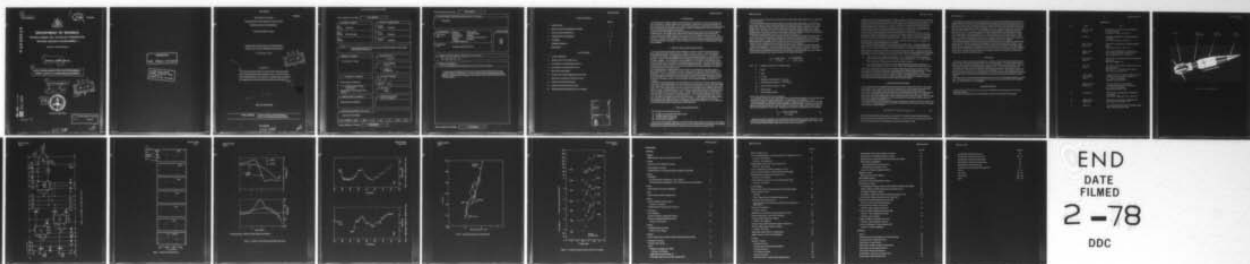
F/O 20/9

UNCLASSIFIED

NL

| OF |

AD  
A048018



END  
DATE  
FILMED  
2-78  
DDC

14

WRE-TR-1828 (W)

12

AR-000-580



AD A 048018

# DEPARTMENT OF DEFENCE

DEFENCE SCIENCE AND TECHNOLOGY ORGANISATION

WEAPONS RESEARCH ESTABLISHMENT ✓

SALISBURY, SOUTH AUSTRALIA

9  
TECHNICAL REPORT, 1828 (W) ✓

6  
ROCKET BORNE OBSERVATION OF ELECTRON DENSITY  
DURING A TRAVELLING IONOSPHERIC DISTURBANCE,

10  
K.H. LLOYD and C.J. BEACH

11  
9 JUN 77

DDC  
RECEIVED  
JAN 4 1978  
REGISTERED  
E

12  
24p.



Approved for Public Release

AU INJ.  
DDC FILE COPY

COPY No. 71

C Commonwealth of Australia  
JUNE 1977

371 700

1/B

**APPROVED  
FOR PUBLIC RELEASE**

**THE UNITED STATES NATIONAL  
TECHNICAL INFORMATION SERVICE  
IS AUTHORIZED TO  
REPRODUCE AND SELL THIS REPORT**

UNCLASSIFIED

AR-000-580

DEPARTMENT OF DEFENCE  
DEFENCE SCIENCE AND TECHNOLOGY ORGANISATION  
WEAPONS RESEARCH ESTABLISHMENT

TECHNICAL REPORT 1828 (W)

ROCKET BORNE OBSERVATION OF ELECTRON DENSITY  
DURING A TRAVELLING IONOSPHERIC DISTURBANCE

K.H. Lloyd and C.J. Beach

DDC  
RECEIVED  
JAN 4 1978  
REGISTERED  
F

SUMMARY

This report presents measurements of the electron density profile made during a period of intense travelling ionospheric disturbance activity. The electron density profile was determined using a swept frequency r.f. impedance probe, and compared with ionograms from an ionosonde located directly below the rocket trajectory.

Approved for Public Release

---

POSTAL ADDRESS: The Director, Weapons Research Establishment,  
Box 21 51, G.P.O., Adelaide, South Australia, 5001.

---

UNCLASSIFIED

371 700

*JB*

DOCUMENT CONTROL DATA SHEET

Security classification of this page

UNCLASSIFIED

1 DOCUMENT NUMBERS

AR  
Number: AR-000-580

Report  
Number: WRE-TR-1828(W)

Other  
Numbers:

2 SECURITY CLASSIFICATION

a. Complete  
Document: Unclassified

b. Title in  
Isolation: Unclassified

c. Summary in  
Isolation: Unclassified

3 TITLE

ROCKET BORNE OBSERVATION OF ELECTRON DENSITY DURING A TRAVELLING IONOSPHERIC DISTURBANCE

4 PERSONAL AUTHOR(S):

K.H. Lloyd and C.J. Beach

5 DOCUMENT DATE:

June 1977

6 6.1 TOTAL NUMBER OF PAGES 24

6.2 NUMBER OF REFERENCES: 11

7 7.1 CORPORATE AUTHOR(S):

Weapons Research Establishment

8 REFERENCE NUMBERS

a. Task: 61/3

b. Sponsoring Agency: RD 73

7.2 DOCUMENT (WING) SERIES AND NUMBER

Weapons Research and Development Wing TR-1828

9 COST CODE:

330897

10 IMPRINT (Publishing establishment):

Weapons Research Establishment

11 COMPUTER PROGRAM(S)  
(Title(s) and language(s))

12 RELEASE LIMITATIONS (of the document):

Approved for Public Release.

12.0	OVERSEAS	NO	P.R.	1	A	B	C	D	E
------	----------	----	------	---	---	---	---	---	---

Security classification of this page:

UNCLASSIFIED

## 13 ANNOUNCEMENT LIMITATIONS (of the information on these pages):

No limitations.

## 14 DESCRIPTORS:

a. EJC Thesaurus  
Terms

Impedance	Plasma (physics)
Thermosphere	Atmospheric models
Sounding rockets	Ionosphere
Observation	Electron density (concentration)
Ionograms	Ionosondes
Ionospheric disturbances	

b. Non-Thesaurus  
Terms

Travelling ionospheric disturbances

## 15 COSATI CODES:

0401  
0402  
2008

## 16 LIBRARY LOCATION CODES (for libraries listed in the distribution):

SW AACR SR SD NL

## 17 SUMMARY OR ABSTRACT:

(if this is security classified, the announcement of this report will be similarly classified)

This report presents measurements of the electron density profile made during a period of intense travelling ionospheric disturbance activity. The electron density profile was determined using a swept frequency r.f. impedance probe, and compared with ionograms from an ionosonde located directly below the rocket trajectory.

## TABLE OF CONTENTS

	Page No.
1. INTRODUCTION	1
2. DESIGN OF THE PLASMA RESONANCE PROBE	1
3. DATA ANALYSIS AND RESULTS	1 - 3
4. COMPARISON WITH IONOGRAMS	3 - 4
5. DISCUSSION	4
ACKNOWLEDGEMENTS	4
REFERENCES	5

## LIST OF FIGURES

1. Cockatoo 3008 payload
2. Principle of operation of the plasma probe
3. Circuit diagram of the swept frequency generator
4. Circuit diagram of the phase sensitive detector
5. Plasma probe telemetered data
6. Example of theoretically calculated plasma probe output
7. High frequency voltage limit of plasma probe output
8. Frequency for plasma probe zero phase
9. Upleg and downleg electron density profiles
10. Travelling ionospheric disturbance observed on ionograms

ACCESSION for	
NTIS	Y on <input checked="" type="checkbox"/>
DDC	B IT S... <input type="checkbox"/>
UNANNOUNCED	<input type="checkbox"/>
JUSTIFICATION	
BY	
DISTRIBUTION/AVAILABILITY NOTES	
Dist.	QUAL
A	

## 1. INTRODUCTION

The impedance of the ionospheric plasma at radio frequencies varies with frequency in a manner characteristic of the density of the plasma. Therefore, a measurement of the ionospheric impedance as a function of altitude enables the electron density profile to be determined. When the electron collision frequency is much smaller than the gyro-frequency, then the resonances and nulls associated with the frequency dependence of impedance show up clearly, and the determination of electron density becomes relatively simple.

Ionograms taken during the flight of an ionospheric impedance probe showed intense T.I.D. (travelling ionospheric disturbance) activity; the impedance probe measured electron density disturbances associated with this activity.

In the next section the principles of operation, and the construction of the impedance probe are discussed. Data obtained from the probe on Cockatoo 4008, fired at Woomera at 14.01 hours C.S.T., on 18 August, 1975, are presented in Section 3. In Section 4, the ionograms obtained during the rocket trial are described, with particular attention paid to the travelling ionospheric disturbances. Finally, the influence of this T.I.D. activity on the observed electron density profile is discussed.

## 2. DESIGN OF THE PLASMA RESONANCE PROBE

Use of the radio frequency dependence of plasma impedance as a technique to measure the ionospheric electron density profile has been made in several ways (see, for example; references 1, 2 and 3). A variety of methods for doing this have been designed. The most satisfactory appears to be that adopted in reference 4. The payload, an r.f. transmitter and receiver, has been designed so that the transmitting element lies between the receiver and the rocket body earth. This ensures that the detected field lines extend beyond the plasma sheath surrounding the rocket into the ambient ionosphere. The receiver-detector circuit was designed to be in the form of a balanced bridge, with the transmitter forming the input to the bridge. By balancing the bridge during assembly of the payload, small departures from the balanced condition could easily be detected, thereby giving great sensitivity. Furthermore, the configuration was designed so the elements are squat (i.e. not long narrow cylinders), thereby approximating spheres, for which the equations describing the impedance are simplest.

In an earlier paper (ref.5), we presented data from an experiment we conducted based on the design concepts of Melzner and Rabben (ref.4). As explained in our paper, we detected spurious resonances, which we attributed to the plasma sheath. In order to eliminate these resonances we redesigned the payload so that the whole of the nose cone constituted the detection element (receiver), the parallel section was the guard ring (transmitter), and the second stage of the rocket made the earth. Figure 1 shows the mechanical configuration of the payload. Although the principles of operation of the plasma probe are as in the previous report, we have reproduced a diagram of it in figure 2 for convenience.

In addition to these physical changes, we also made modifications to the electronics. The swept frequency generator, shown in figure 3, was redesigned using the sine wave generator XR 205 in place of beat oscillators. The output voltage of the frequency generator was reduced to 0.3 V p-p. This was to minimise disturbance to the ambient electron density by the r.f. field. Also, a phase sensitive detector (P.S.D.) was added so that phase as well as amplitude of the detected signal was recorded. This made interpretation of the data easier, as the phase goes through zero at the plasma resonance.

The circuit diagram for the P.S.D. is shown in figure 4. The phase sensitive detector compares the phase difference between the outputs of the receiver and sweep frequency generator. Two F.M. limiting amplifiers X1 and X2 are used to limit the inputs to the P.S.D. (X4) to a constant amplitude of 1.5 V for a receiver output voltage range of 50 mV to 3.5 V. The output from amplifier X3 is fed directly into the telemetry. A  $+90^\circ$  phase difference voltage at TN3 and TN4 produces an output voltage from X3 of +5 V, falling to +2 V when the input voltages are  $-90^\circ$  out of phase. The circuit diagram of the differential amplifier was unchanged from that shown in reference 5, so it is not shown here. It detected the voltage difference across the bridge, as shown in figure 2(a).

## 3. DATA ANALYSIS AND RESULTS

The following data were telemetered to ground:

- (1) The high and low gain differential amplifier outputs
- (2) The phase sensitive detector output
- (3) The sweep frequency voltage ramp
- (4) The +0 V and +5 V references

The data were time multiplexed, modulating an A.M./F.M. 465 MHz telemetry sender with 24 channels. The amplitude and phase data were each allocated several channels in order to obtain maximum detail of the resonances, whereas sufficient information on the voltage ramp and reference voltages was obtained by using only one channel for each.



Figure 5 gives portions of the telemetered data, showing the low gain amplifier, phase sensitive detector, voltage ramp, and reference voltages.

It is seen that below 100 km there is very little variation in the detector output with frequency. This is because at these altitudes the electron collision frequency was high, and this damped out response of the plasma to the r.f. signal. However, above 100 km this effect of the electron collisions decreased rapidly and the r.f. dependence of the plasma impedance showed up clearly. There is a small systematic difference between multiplex channels on the low gain amplifier output. This is thought to be due to r.f. interference. Despite considerable care in the design of electronic packaging to prevent unwanted r.f. pickup, it proved impossible to eliminate it altogether. However, since the difference in signal between channels remained constant in time, it was possible to correct for it.

In the analysis of the data to obtain the electron density profile, we attempted to fit the observed variation of impedance with frequency to cold plasma theory (which proved to be difficult, as explained below). This method gives absolute electron density. We also obtained the small scale variation in electron density with altitude by measuring two limiting parameters in the impedance curves - the high frequency limit to the differential amplifier output, and the frequency at which the phase indicated by the phase sensitive detector went through zero.

Reference 6 gives a comparison of various theoretical expressions for the r.f. impedance of a plasma and discusses possible payload configurations. The capacitor consisting of the rocket body and nose cone as plates and ionospheric plasma as medium (P in figure 2(a)), has an impedance which depends on the physical configuration. However, by considering the potential distribution around a point charge immersed in an anisotropic plasma, it is shown in reference 7 that the general expression for the frequency dependence of the (complex) capacitance is

$$\frac{C}{C_0} = \frac{1 - (X/U) - (Y/U)^2}{1 - (Y/U)^2} \cdot \sqrt{1 + \frac{(X/U)(Y/U)^2 G}{1 - (X/U) - (Y/U)^2}} \quad (1)$$

where  $C_0$  = capacitance in the absence of ionospheric plasma

$$X = (f_N/\Gamma)^2$$

$$Y = (f_B/\Gamma)$$

$$U = 1 - i\nu/2\pi f$$

$C$  = capacitance, in the ionosphere, at a frequency  $f$

$f_N$  = ionospheric plasma frequency ( $= \sqrt{Ne^2/2\pi m\epsilon_0}$ )

$f_B$  = electron cyclotron frequency ( $= eB/m$ )

$N$  = electron density

$\nu$  = electron collision frequency,

and the other symbols have their conventional meanings.

$G$  is a parameter, of the order of unity, which depends both on the geometrical configuration, and on the angle between the axis of the capacitor and the earth's magnetic field. For example, for an infinite cylinder  $G = \sin^2\theta$ .

The expression, equation 1, applies to a cold anisotropic plasma. However, as is shown in reference 6, it is also valid for electron temperatures less than 3000°K, which is applicable to the lower ionosphere. If the second term under the square root sign is much less than unity, which is expected in the region near the upper hybrid resonance frequency, the root may be expanded in a Taylor's series. Retaining terms to first order of small quantities gives the expression:

$$\frac{C}{C_0} = 1 - \frac{(X/U)(1 - (Y/U)^2) G/2}{(1 - (Y/U)^2)} \quad (2)$$

This equation is the one commonly quoted for a parallel plate capacitor(ref.8), and an infinite cylinder(ref.9). It has the benefit of being easily manipulated to give the unknown quantities in terms of measured variables. However, since our sweep frequency passes through the upper hybrid resonance, we have used equation 1.

Using equation 1 for the frequency dependence of the plasma impedance, we have calculated values for the amplitude and phase of the output voltage across the bridge for different values of electron density and collision frequency. These calculations required the values of impedance for the circuit elements, and of the physical capacitance between, for example, the nose cone and rocket body. In some cases it was difficult to measure impedance with the payload completely assembled, and it was necessary to estimate a correction to the measured value. Another cause of error was the parameter  $G$ , which was not totally independent of  $\theta$ . However, it was found that the output curves were insensitive to variations of circuit impedance and of  $G$ , within their expected uncertainties.

When we were curve fitting the data, we found that the required value of electron collision frequency was several times greater than expected. This has been noted before (see, for example, reference 10), and is due to the varying electron density across the plasma sheath surrounding the vehicle. We also found that, to get profiles which agreed with the data, we had to use a value for the physical capacitance ( $C_0$ ) between detector and body, much larger than the measured value. The reason for this is not clear. Because of the design of the experiment, it is unlikely to be caused by parallel and shunt capacitative effects of the sheath.

Figure 6 shows an example of calculated values for the output of the plasma probe. Comparing with the data on figure 5 shows that only fair agreement was obtained with the observations. The fact that we were unable to find values for  $f_N$  and  $\nu$  which gave good agreement between the calculations and observations is likely to stem from the simplified manner in which we have modelled the circuit elements comprising the bridge. It is unfortunate that such an approach was not entirely satisfactory, since it would be extremely difficult to estimate parameters in a more detailed circuit evaluation. However, as mentioned earlier, variations in electron density can be determined by two methods:

- (a) The asymptotic value of voltage at high frequencies. For r.f. much greater than the gyro- and plasma frequencies, the plasma capacitance varies with electron number density as  $C/C_0 = 1-X$ . As seen in figure 7, which plots this data for the upleg, this method gave good detail on structure.
- (b) Zero crossing of phase. The frequency at which phase goes through zero, should be an indication of number density, independent of the rocket altitude. Figure 8 plots the upleg data obtained by this method.

The validity of these methods, which have the disadvantage of only giving relative instead of absolute values for electron density, was confirmed by running the computer program for several values of plasma frequency. A further indication that the two methods are measuring the same thing is that the measured profiles are very similar.

Figure 9 plots the derived electron density as a function of attitude. The small scale variations in electron density were obtained as discussed above, and these were added to the gross profile determined from scaling the ionograms. It is seen that the up and downleg profiles are similar in shape, but shifted in altitude.

#### 4. COMPARISON WITH IONOGRAMS

Figure 10 gives tracings from ionograms taken over a period of half an hour either side of the firing. Unfortunately the ionograms were low in contrast, so they could not be reproduced here. Only the ordinary ray traces have been shown, to make the figure clearer. For the same reason, alternate ionograms are drawn with a thicker line.

It is seen that, over the period covered by the ionograms, a travelling ionospheric disturbance (T.I.D.) had progressed down from the middle of the F1 region to the E region. These perturbations in electron density are attributed to internal gravity waves, which have the property of downward phase progression as they move upward. They are thought to be mainly produced either by magnetic storm activity, particularly in the auroral regions from where they move poleward, or by weather systems such as fronts.

The small scale structure of electron density measured by the plasma probe is consistent with the T.I.D. activity shown on the ionogram. The vertical and horizontal wave number of internal gravity waves ( $k_z, k_x$ ) are related to their angular frequency ( $\omega$ ) by the expression(ref.11):

$$(\omega^2 - \omega_a^2) \omega^2 / C^2 - \omega^2 (k_x^2 + k_z^2) + \omega_g^2 k_x^2 = 0 \quad (3)$$

where  $C$  is the acoustic velocity, and  $\omega_a$  and  $\omega_g$  are the acoustic cut-off and Brunt-Vaisala frequencies respectively.

Using values of these three parameters typical of the E region,  $k_z = 4 \times 10^{-4} \text{ m}^{-1}$  (from the rocket data) and a period of one hour (from the T.I.D.'s on the ionograms) gives a horizontal wavelength of 150 km.

An alternative way to estimate a limit to horizontal wavelength is from the vertical displacement of the profiles on the up and downlegs. Since the times of the up and downleg parts of the trajectory differ by only about 2 min, which is a small fraction of the period of the wave, the wave will not have travelled far during this time, and displacement of the up and downleg profiles is mainly due to change in the horizontal phase. The greatest change will occur when the ground path of the rocket coincides with the direction of propagation of the wave. This gives an upper limit to the horizontal wavelength, which we will now calculate. At 120 km altitude the vertical displacement between up and downleg profiles is about 5 km, i.e. a third of a wavelength. The horizontal separation of the up and downlegs at this altitude is 25 km, which gives a horizontal wavelength of 75 km. This is rather less than the other estimate, however a mean value of 100 km, with a corresponding period of 35 min, still lies within the uncertainty of both methods. Internal gravity waves with these characteristics are expected at these altitudes as they have long enough vertical wavelength not to be dissipated, neither are they reflected to ground by the temperature structure at the mesosphere.

The approximate agreement between the horizontal wavelength determined by the two methods, the second of which gives an upper limit, indicates that the direction of propagation of the wave must lie approximately along the rocket's ground trajectory. Since the downleg profile was lower than the upleg, and since the phase of internal gravity waves descends with upward propagation, this suggests that the wave had come from the South East. As we have an indication of the direction from which the waves came, and since the T.I.D.'s were so strong, we had hoped to be able to identify a source of them. However, there had not been any strong magnetic storms for several days prior to firing, and the weather patterns showed no strong frontal activity.

## 5. DISCUSSION

Although the impedance probe functioned satisfactorily, problems were experienced in fitting the observed variation in detector output with calculations using the theory for a cold anisotropic plasma. The values for effective electron collision frequency, and detector capacitance, required to give a fit to the data were greater than expected. The former was attributed to the effect of the plasma sheath surrounding the vehicle; no reason could be given for the latter.

The voltage limit at high frequency, and frequency at which phase went through zero, gave consistent profiles for the small scale variation of electron density. They gave a vertical wavelength of 15 km. Using the dispersion equation for internal gravity waves, and a period of 35 min (the period of T.I.D. activity observed on the ionograms) gave a horizontal wavelength of 100 km. This is compatible with the shift in altitude between the upleg and downleg electron density profiles.

The deduced scale of the internal gravity waves which produced the T.I.D.'s on the ionograms lies within the expected range. Unfortunately, there was no strong magnetic storm or weather activity previously which could be ascribed as their source, which as shown to lie to the South East.

## ACKNOWLEDGEMENTS

We wish to thank A.D. Hind and G. O'Connor for many useful discussions during this project, and C.H. Low for providing the ionograms.

The Cockatoo rocket was fired as part of the Department of Defence upper atmosphere research project.

## REFERENCES

- | No. | Author                                    | Title   |
|-----|---|---|
| 1   | Jackson, J.E. and Kane, J.A.              | "Measurement of ionospheric electron densities using R.F. probe technique"<br>J. Geophys. Res. Vol. <u>64</u> , p.1074, 1959  |
| 2   | Power, K.                                 | "Ionosphären-messungen bei zwei Raketen-Aufstiegen in der Sahara"<br>Zeit. Fur Geophys. Vol. <u>32</u> , p.409, 1966  |
| 3   | Miller, E.K. and Schutte, H.K.            | "Results from a swept-frequency ionospheric impedance probe"<br>Planet. Space Sci. Vol. <u>22</u> , p.1017, 1974  |
| 4   | Melzner, F. and Rabben, H.                | "Electronendichte-Messungen in der Ionosphäre mit einer neuartigen Hoch frequenz-Impedanz sonde"<br>Zeit. fur Geophysik Vol. <u>36</u> , p.135, 1970                            |
| 5   | Lloyd, K.H. and Beach, C.J.               | "Results from a rocket-borne swept-frequency ionospheric plasma probe"<br>WRE-TN-978 (WR&D), 1973   |
| 6   | Kist, R. and Neske, E.                    | "Die impedanz sonde der Arbeit grupper fur Physikalische Weltraumforschung"<br>BMFT-FBM 73-71. Arbeitsgruppe fur Physikalische Weltraumforschung, Freiburg, 1973                |
| 7   | Storey, L.R.O., Aubry, M.P. and Meyer, P. | "A quadrupole probe for studying ionospheric resonances. In "Plasma waves in space and in the laboratory"<br>Ed. J. Thomas and B. Landmark.<br>Edinburgh University Press, 1969 |
| 8   | Balamin, K.G. and Oksiutik, G.A.          | "R.F. probe admittance in the ionosphere"<br>In "Plasma waves in space and in the laboratory"<br>Ed. J. Thomas and B. Landmark<br>Edinburgh University Press, 1969              |
| 9   | Domorazek, G.                             | "Impedanzsonde zur Messung der Electronendichte in der Ionosphäre"<br>Electrotechnik u. Maschinen Vol. <u>92</u> , p.203, 1971  |
| 10  | Miller, E.K. and Schulte, H.F.            | "Results from a swept frequency-ionospheric probe"<br>Planet. Space Sc. Vol. <u>22</u> , p.1017, 1974   |
| 11  | Hines, C.O.                               | "Internal atmospheric gravity waves at ionospheric heights"<br>Canad. J. Phys. Vol. <u>38</u> , p.1441, 1960  |

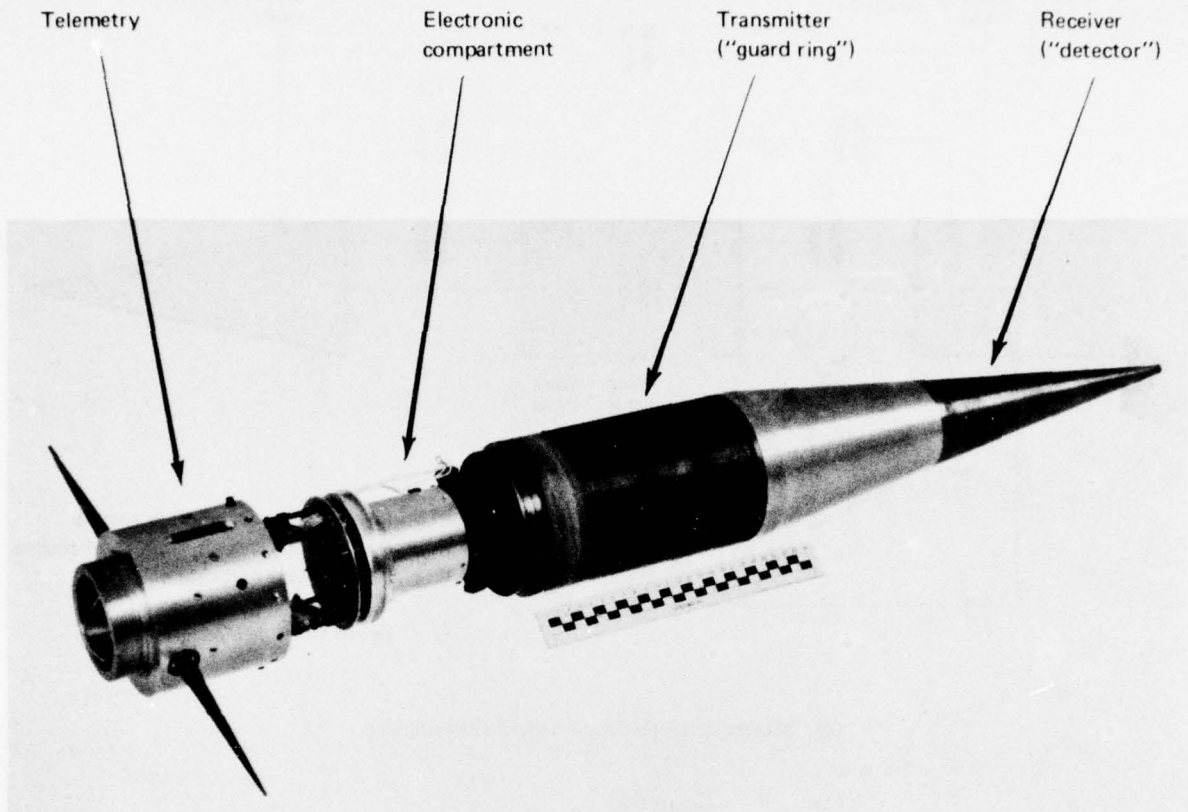
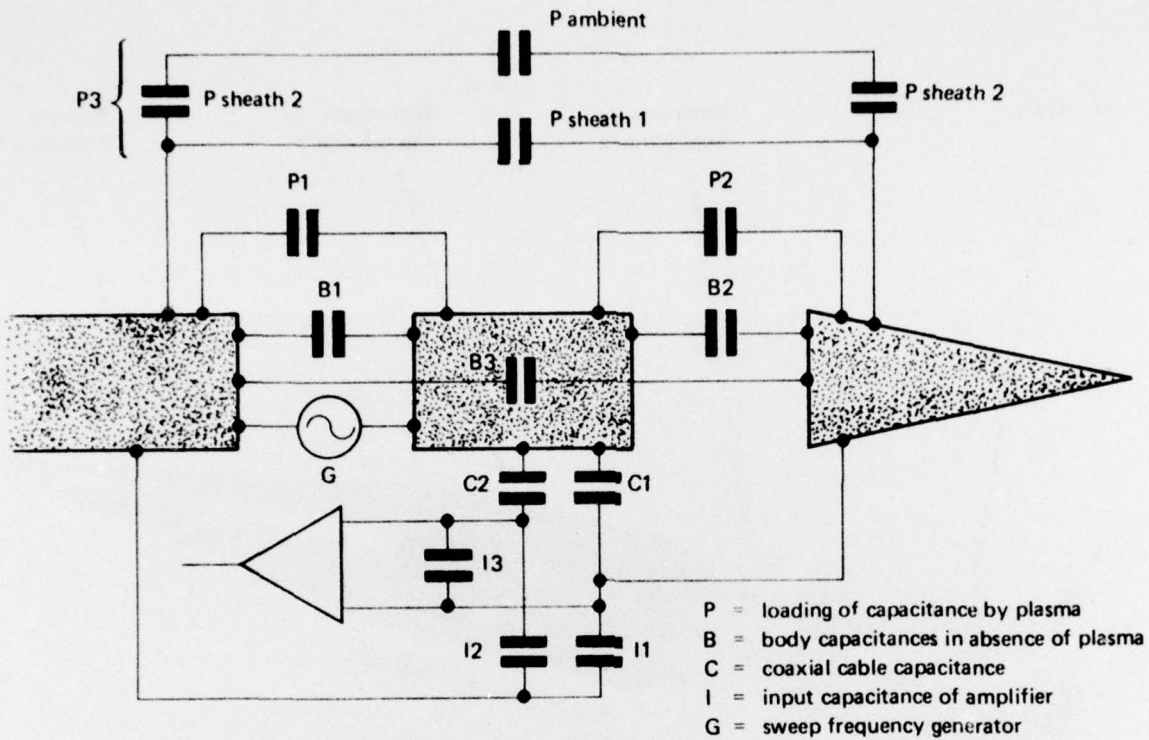
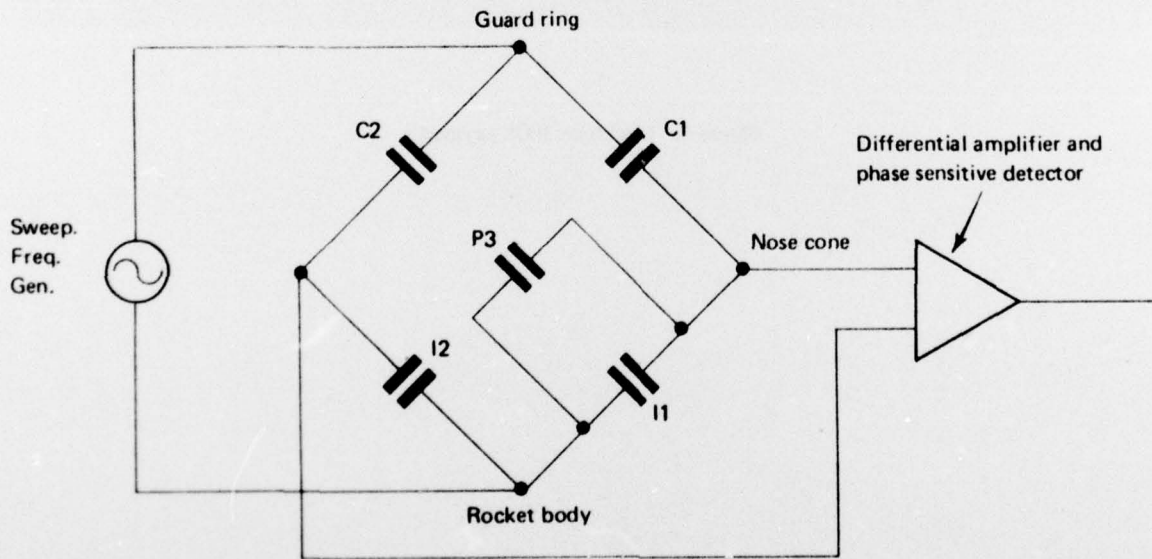


Figure 1. Cockatoo 3008 payload



(a) Schematic representation of the impedances



(b) Simplified equivalent bridge circuit.  
 The coaxial cable, C1, is loaded with a variable capacitor adjusted before flight.

Figure 2. Principle of operation of the plasma probe

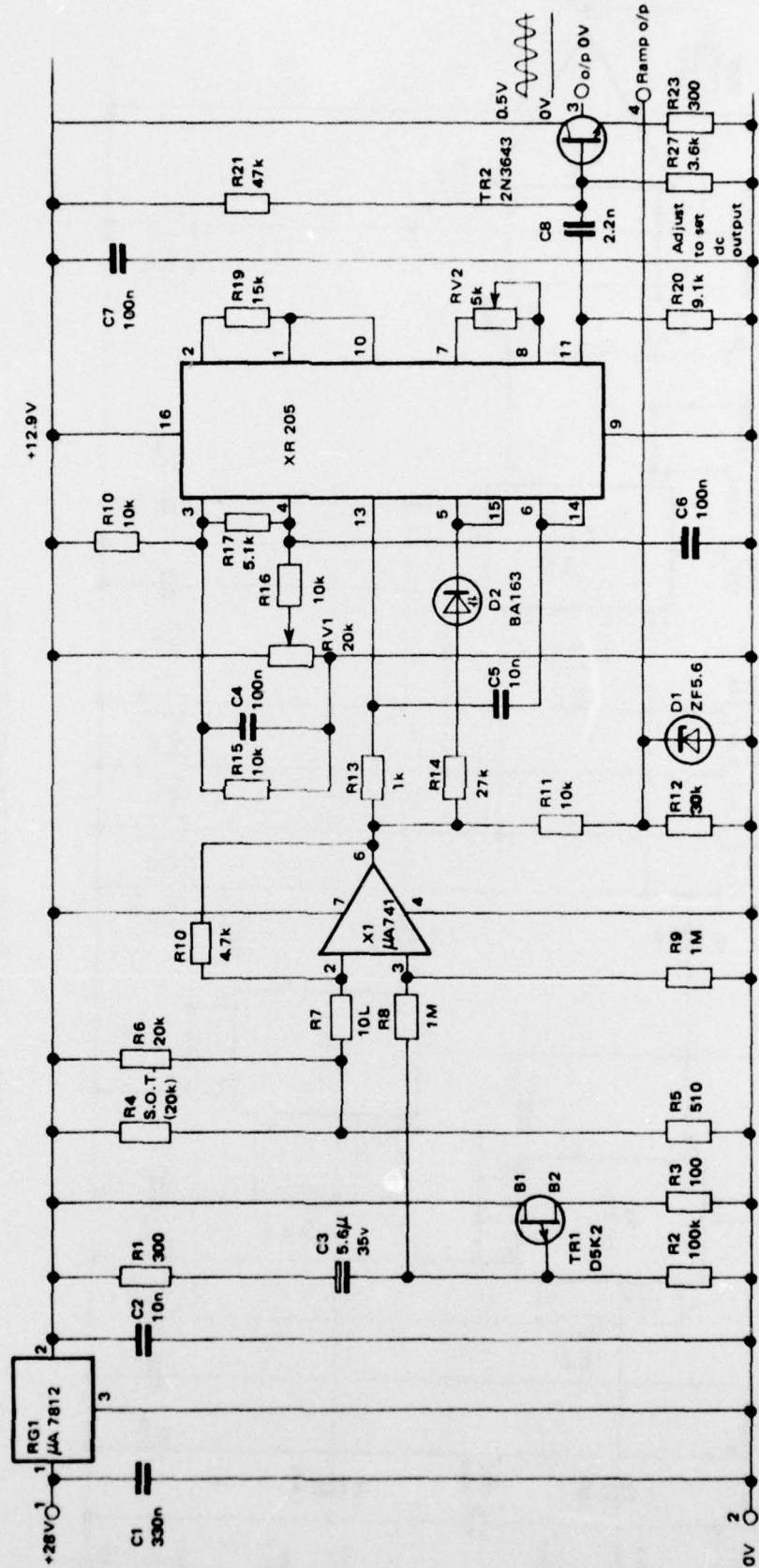


Figure 3. Circuit diagram of the swept frequency generator

WRI-TR-182M(W)  
 Figure 4

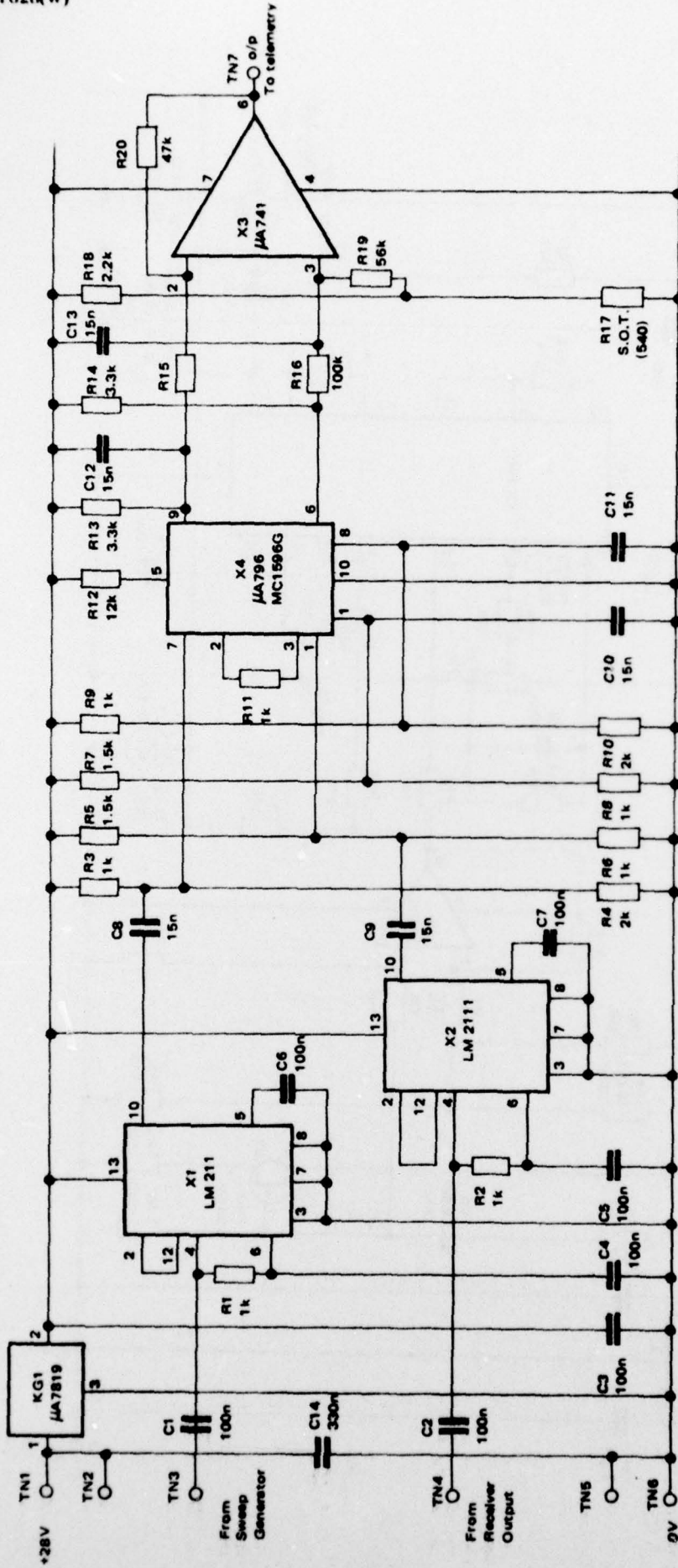


Figure 4. Circuit diagram of the phase sensitive detector



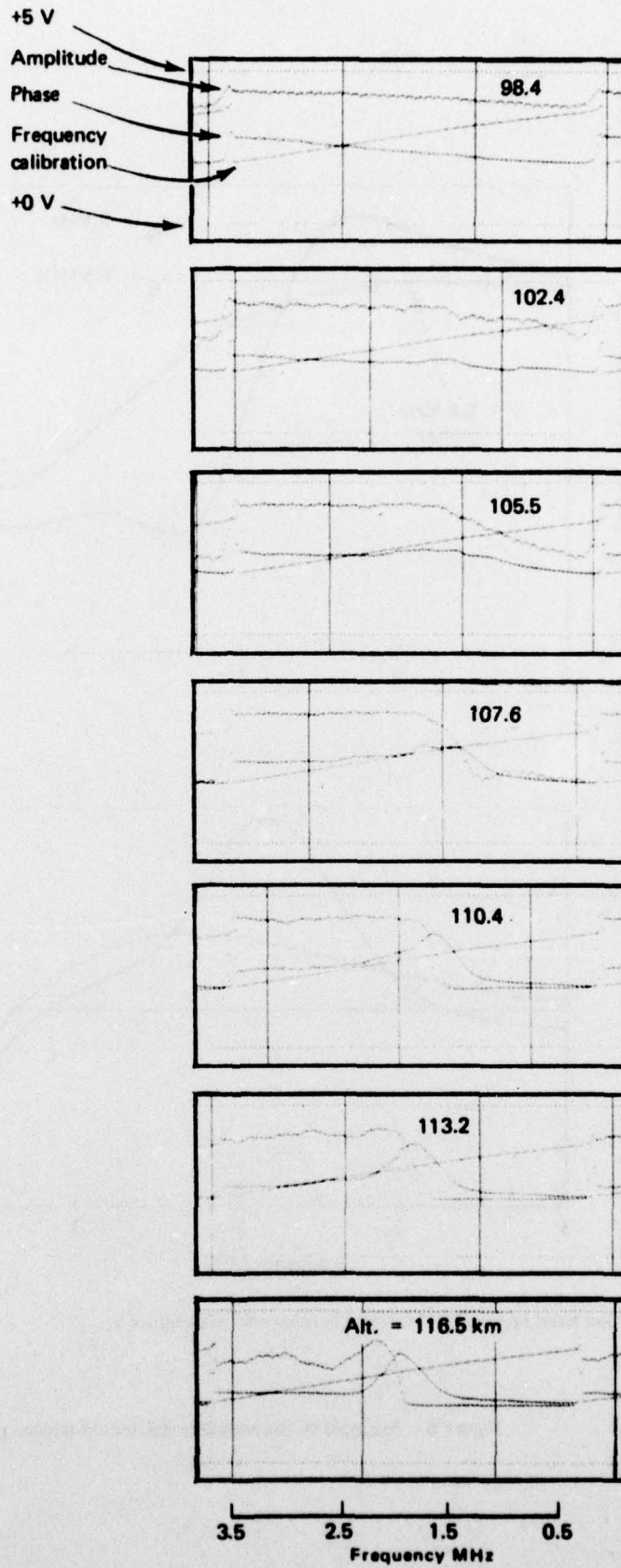
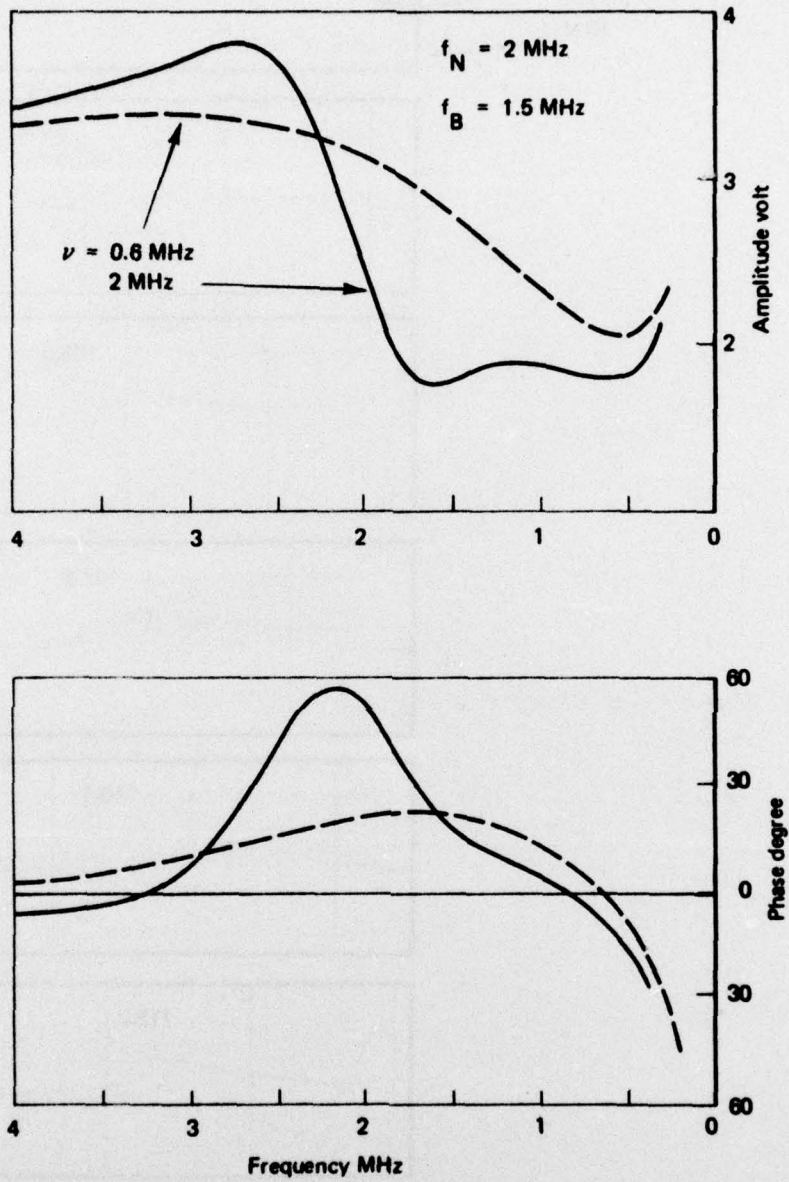


Figure 5. Plasma probe telemetered data



The scales have been reversed to facilitate comparison with figure 5.

Figure 6. Example of theoretically calculated plasma probe output

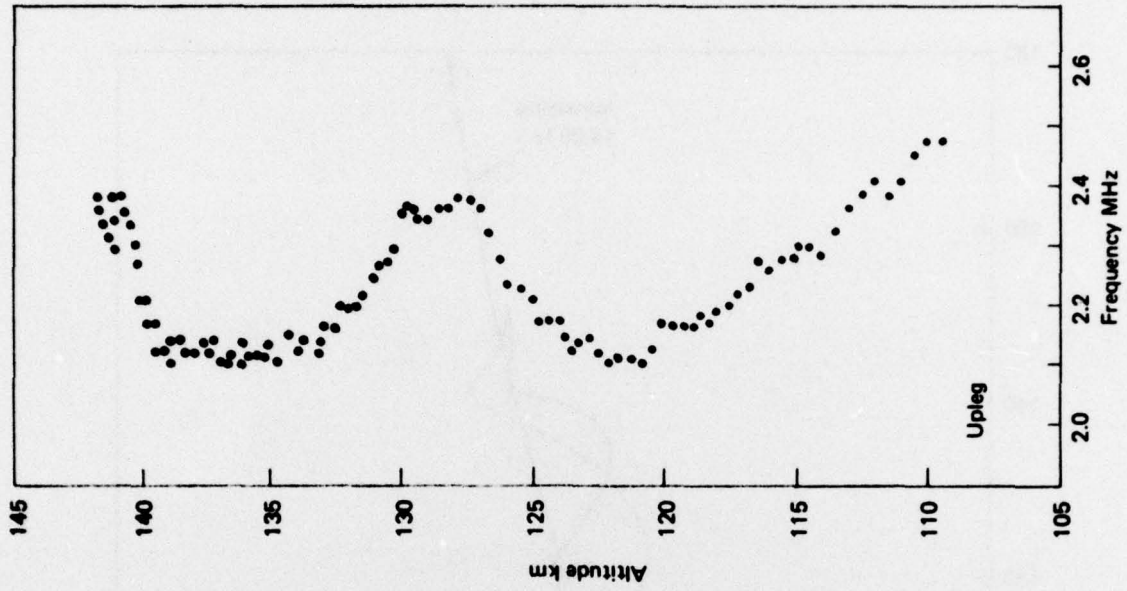


Figure 8. Frequency for plasma probe zero phase

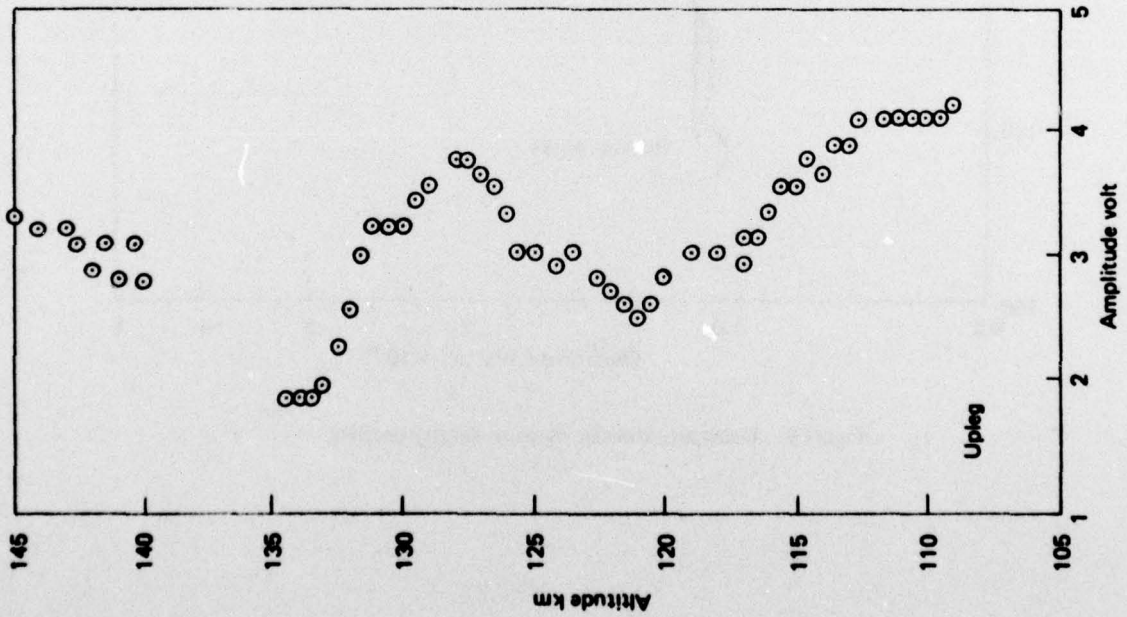


Figure 7. High frequency voltage limit of plasma probe output

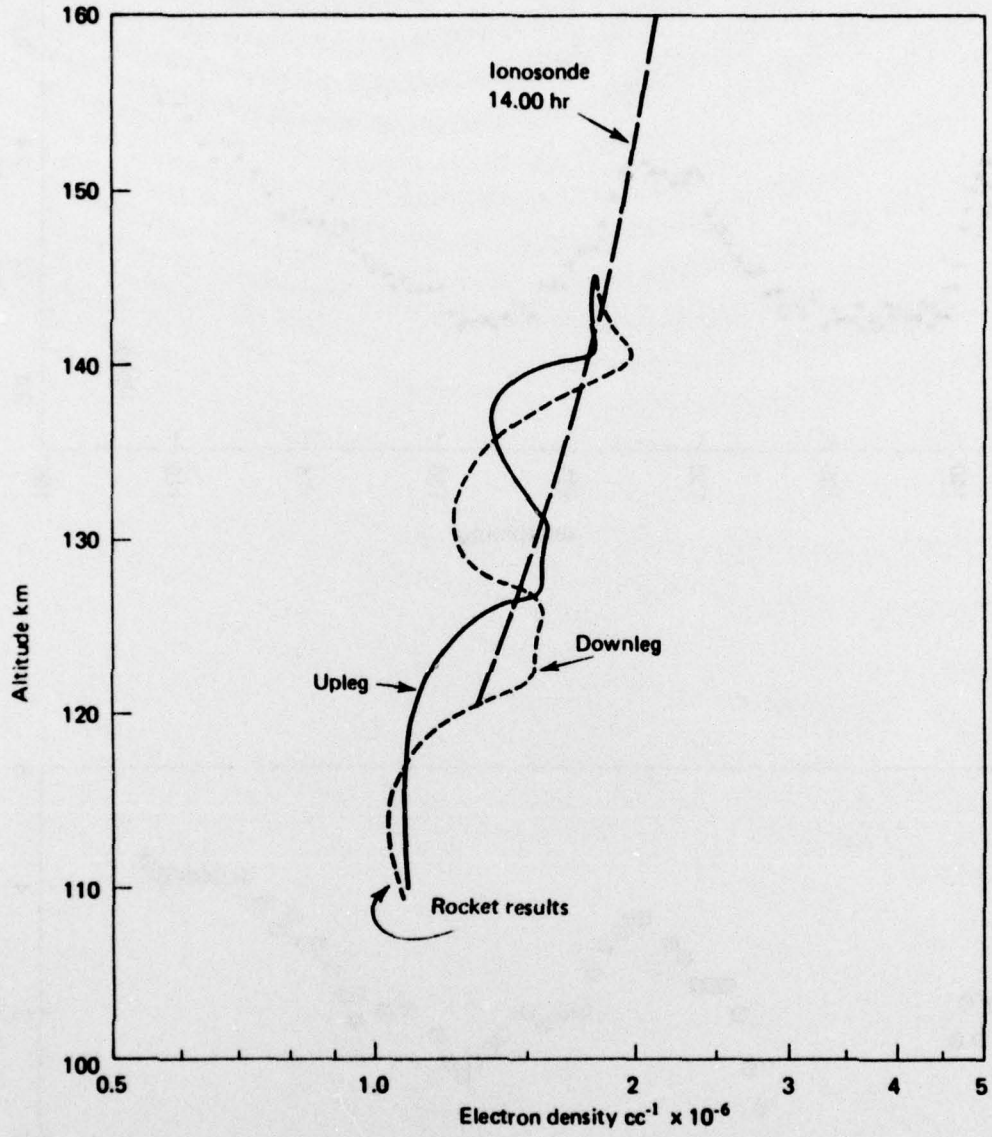


Figure 9. Upleg and downleg electron density profiles.

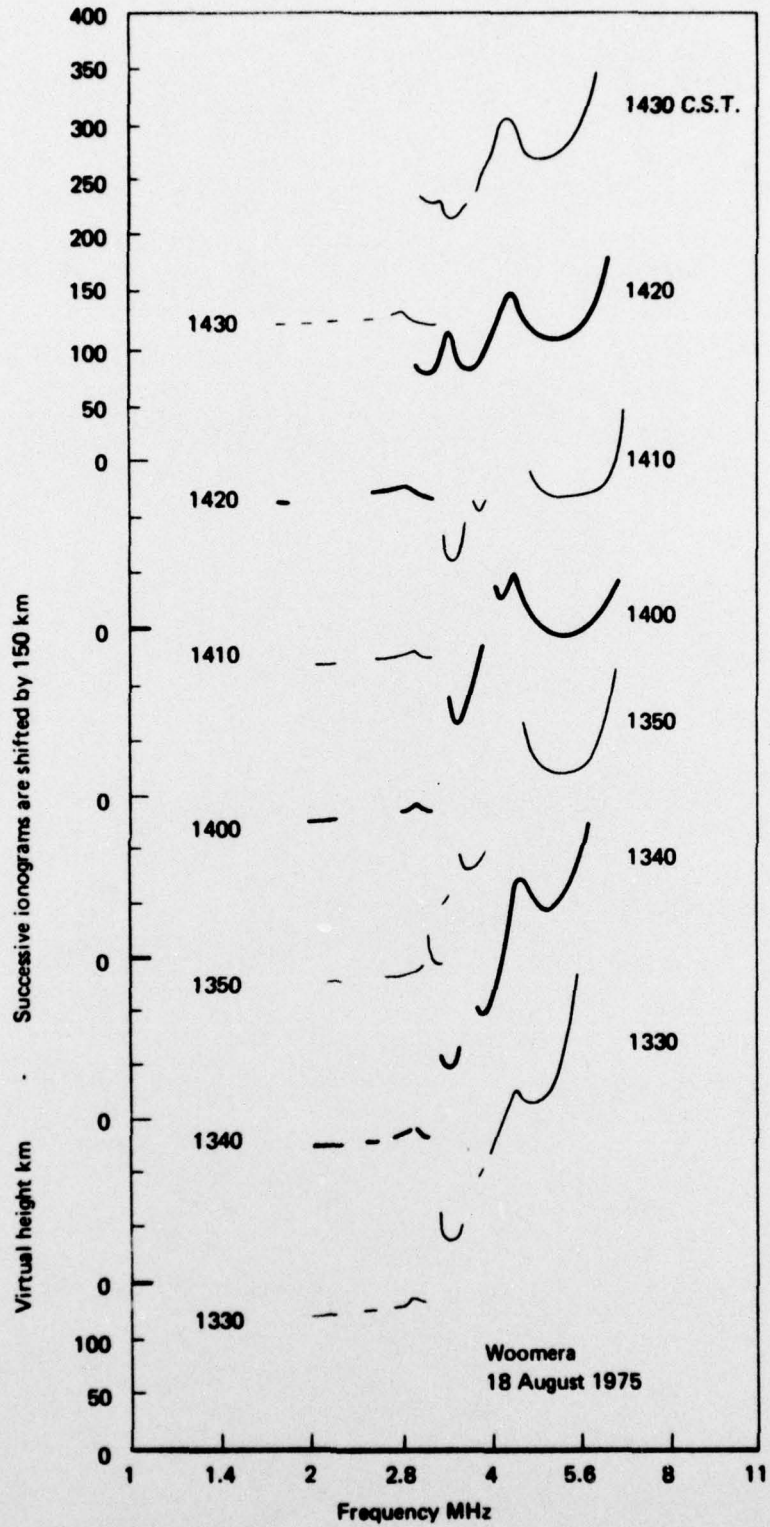


Figure 10. Travelling ionospheric disturbance observed on ionograms

## DISTRIBUTION

## EXTERNAL

Copy No.

## In Belgium

Belgian Institute for Space Aeronomy, Brussels, B-1180 1

## In Canada

University of Toronto, Department of Physics 2

## In Federal Republic of Germany

Max-Planck Institute for Extraterrestrial Physics, Garching, b. Munich, 8046 3

## In France

## ELDO/ESRO

Group de Recherches Ionospheriques, C.N.R.S., Orleans 4

Group de Recherches Ionospheriques, C.N.E.T., Station Pierre Le Jay, Garchy (Nievre) 5

## In India

Physical Research Laboratories, Ahmedabad,9 6

## In Italy

Instituto di Fisica Atmosfera, Bologna, 40126 7

## In Japan

Institute of Physics, University of Tokyo 8

(Attention: J. Nakamura)

Ionospheric Research Laboratory, Kyoto University 9

## In New Zealand

D.S.I.R. Wellington 10

University of Canterbury, Department of Physics 11

University of Auckland, Radio Research Centre  
(Attention: Mr D.A. Price) 12

## In Norway

The Auroral Observatory, Tromso  
(Attention: Mr O. Harang) 13

## In Pakistan

Director, Pakistan Space and Upper Atmosphere Research Committee, Karachi 14

## In United States of America

Counsellor, Defence Science 15

## N.A.S.A.

Headquarters, Washington D.C., 20546 16

(Attention: Mr M. Dubin) 17

Langley Research Centre, Hampton, Va 17

Goddard Space Flight Centre, Greenbelt, Maryland, 20771 18

	Copy No.
Library of Congress, U.S.A.	19
Air Force Cambridge Research Laboratories, Hanscom Field, Massachusetts, 01730	
(Attention: Dr D. Golomb)	20
(Attention: Dr M.A. MacLeod)	21
Georgia Institute of Technology, Atlanta, Georgia, 30332	
(Attention: Dr R.G. Roper)	22
G.C.A. Technology Division, Bedford, Massachusetts, 01730	23
National Centre for Atmospheric Research, Boulder Colorado, 80302	24
Sandia Laboratories, Albuquerque, New Mexico, 87115	
(Attention: Dr L. B. Smith)	25
Aeronomy Laboratory, University of Illinois, Urbana, Illinois, 61801	
(Attention: E.A. Mechtly)	26
<b>In United Kingdom</b>	
Defence Science and Technology Representative, Australia House, London	27
Ministry of Defence, London	
AD/TGW2	28
TGW25, Weapons Research Establishment Representative	29
The Chairman, Rockets Working Group	
<i>Design Experiments Sub-Committee of the British National Committee for Space Research</i>	30
Royal Aircraft Establishment	
(Attention: Library)	31
Admiralty Centre for Scientific Information and Liaison, London	32
National Lending Library of Science and Technology	33
University of Belfast, Department of Physics	
(Attention: Dr A. Dalgarno)	34
University College of Wales, Department of Physics, Aberystwyth	35
University College London, Department of Physics	
(Attention: Dr D. Rees)	36
Mullard Space Sciences Laboratory, Dorking, Surrey	37
Appleton Laboratory, Ditton Park, Slough, Bucks	38
<b>In Australia</b>	
Department of Defence	
Chief Defence Scientist	39
Controller, Policy and Program Planning Division	40
Army Scientific Adviser	41
Air Force Scientific Adviser	42
Naval Scientific Adviser	43
Executive Controller, Australian Defence Scientific Service	44

	Copy No.
Superintendent, Defence Science Administration Division	45
Superintendent, Central Studies Establishment, Canberra	46
Assistant Secretary, Defence and Information Services (for microfilming)	47
Defence Library, Campbell Park	48
Aeronautical Research Laboratories, Library	49
Materials Research Laboratories, Library	50
Director, Joint Intelligence Organisation (DDSTI)	51
Department of Science	52
Director, Antarctic Division, Melbourne	53
Head of BDRSS, Salisbury	54
N.A.S.A. Senior Scientific Representative, Canberra	55
National Library, Canberra	56
United Kingdom, for Ministry of Defence, Defence Research Information Centre(DRIC)	57
Canada, for Ministry of Defence, Defence Science Information Service	58
New Zealand, for Ministry of Defence	59
United States, for Department of Defense, Defense Documentation Center	60 - 71
C.S.I.R.O. Division of Physics, Narrabri, New South Wales, 2390	72
Flinders University, Bedford Park, South Australia, 5042	
(Attention: Head of School of Physical Sciences)	73
La Trobe University, Bundoora, Victoria, 3083	
(Attention: Head of Department of Physics)	74
University of Adelaide, Adelaide, South Australia, 5000	
(Attention: Head of Department of Physics)	75
(Attention: Dr R.A. Vincent)	76
University of Melbourne, Parkville, Victoria, 3052	
(Attention: Head of Department of Physics)	77
University of Queensland, St. Lucia, Queensland, 4067	
(Attention: Professor D. Whitehead)	78
<b>INTERNAL</b>	
Director	79
Chief Superintendent, Weapons Research and Development Wing	80
Chief Superintendent, Applied Physics Wing	81
Superintendent, Aerospace Division	82
Superintendent, Propulsion and Marine Physics Division	83
Superintendent, Systems Assessment Division	84
Superintendent, Weapons Systems Division	85
Principal Officer, Combustion and Explosives Group	86
Principal Officer, Field Experiments Group	87



	Copy No.
Principal Officer, Flight Research Group	88
Principal Officer, Ionospheric Studies Group	89 - 91
Principal Officer, Tropospheric Studies Group	92
Principal Officer, Underwater Detection Group	93
Principal Officer, Marine Physics Group	94
Principal Officer, Terminal Guidance Systems Group	95
Authors	96 - 97
A.D. Library	98 - 99
W.R.E. Library	100 - 101
Spares	102 - 107